

**Influence of Tile Geometry on the Dynamic Fracture of  
Silicon Carbide (SiC)**

**by Jacqueline T. Le and Shane D. Bartus**

**ARL-TR-6861**

**March 2014**

## **NOTICES**

### **Disclaimers**

The findings in this report are not to be construed as an official Department of the Army position unless so designated by other authorized documents.

Citation of manufacturer's or trade names does not constitute an official endorsement or approval of the use thereof.

Destroy this report when it is no longer needed. Do not return it to the originator.

# **Army Research Laboratory**

Aberdeen Proving Ground, MD 21005-5066

---

---

**ARL-TR-6861**

**March 2014**

---

## **Influence of Tile Geometry on the Dynamic Fracture of Silicon Carbide (SiC)**

**Jacqueline T. Le**  
George Washington University

**Shane D. Bartus**  
Weapons and Materials Research Directorate, ARL

<b>REPORT DOCUMENTATION PAGE</b>			<i>Form Approved</i> <b>OMB No. 0704-0188</b>		
Public reporting burden for this collection of information is estimated to average 1 hour per response, including the time for reviewing instructions, searching existing data sources, gathering and maintaining the data needed, and completing and reviewing the collection information. Send comments regarding this burden estimate or any other aspect of this collection of information, including suggestions for reducing the burden, to Department of Defense, Washington Headquarters Services, Directorate for Information Operations and Reports (0704-0188), 1215 Jefferson Davis Highway, Suite 1204, Arlington, VA 22202-4302. Respondents should be aware that notwithstanding any other provision of law, no person shall be subject to any penalty for failing to comply with a collection of information if it does not display a currently valid OMB control number. <b>PLEASE DO NOT RETURN YOUR FORM TO THE ABOVE ADDRESS.</b>					
<b>1. REPORT DATE (DD-MM-YYYY)</b> March 2014		<b>2. REPORT TYPE</b> Final		<b>3. DATES COVERED (From - To)</b> August 2012	
<b>4. TITLE AND SUBTITLE</b> Influence of Tile Geometry on the Dynamic Fracture of Silicon Carbide (SiC)			<b>5a. CONTRACT NUMBER</b> W911NF-10-2-0076		
			<b>5b. GRANT NUMBER</b>		
			<b>5c. PROGRAM ELEMENT NUMBER</b>		
<b>6. AUTHOR(S)</b> Jacqueline T. Le* and Shane D. Bartus			<b>5d. PROJECT NUMBER</b>		
			<b>5e. TASK NUMBER</b>		
			<b>5f. WORK UNIT NUMBER</b>		
<b>7. PERFORMING ORGANIZATION NAME(S) AND ADDRESS(ES)</b> U.S. Army Research Laboratory ATTN: RDRL-WMP-E Aberdeen Proving Ground, MD 21005-5066			<b>8. PERFORMING ORGANIZATION REPORT NUMBER</b> ARL-TR-6861		
<b>9. SPONSORING/MONITORING AGENCY NAME(S) AND ADDRESS(ES)</b>			<b>10. SPONSOR/MONITOR'S ACRONYM(S)</b>		
			<b>11. SPONSOR/MONITOR'S REPORT NUMBER(S)</b>		
<b>12. DISTRIBUTION/AVAILABILITY STATEMENT</b> Approved for public release; distribution is unlimited.					
<b>13. SUPPLEMENTARY NOTES</b> *George Washington University, 2121 I St NW, Washington, DC 20052					
<b>14. ABSTRACT</b> Ceramic materials have been investigated for use in armor systems for over 40 years. The purpose of this study is to see how different sized ceramic tiles react when struck by a projectile. This study examined the response of 19-mm-thick silicon carbide-X1 (SiC-X1) ceramic tiles that were bonded to 12.7-mm-thick polycarbonate and impacted by 12.7-mm-diameter tungsten carbide (WC) spheres. Three different sized SiC-X1 hexagonal tiles were used: 50-mm flat-to-flat, 75-mm flat-to-flat, and 100-mm flat-to-flat. A light gas gun was used to propel the spheres at a nominal velocity of 440 m/s <sup>-1</sup> . A high-speed camera was set up to record the back surface of the ceramic and Image-Pro Plus 6.3 was used to analyze the footage from the high-speed camera and quantify failure and fracture of the ceramic as a function of the tile geometry. The 75- and 50-mm flat-to-flat tiles exhibited a 42% and 205% increase in crack density, respectively, over the 100-mm flat-to-flat hexagonal tile baseline.					
<b>15. SUBJECT TERMS</b> ceramics, ballistic impact, SiC-X1, silicon carbide, dynamic fracture					
<b>16. SECURITY CLASSIFICATION OF:</b>			<b>17. LIMITATION OF ABSTRACT</b>	<b>18. NUMBER OF PAGES</b>	<b>19a. NAME OF RESPONSIBLE PERSON</b> Shane D. Bartus
<b>a. REPORT</b>	<b>b. ABSTRACT</b>	<b>c. THIS PAGE</b>			<b>19b. TELEPHONE NUMBER (Include area code)</b>
Unclassified	Unclassified	Unclassified	UU	28	410-278-6012

---

# Contents

---

<b>List of Figures</b>	<b>iv</b>
<b>List of Tables</b>	<b>iv</b>
<b>Acknowledgments</b>	<b>v</b>
<b>1. Introduction</b>	<b>1</b>
<b>2. Materials and Methods</b>	<b>2</b>
2.1 Target Setup .....	2
2.2 Light Gas Gun Setup .....	3
2.3 Data Analysis .....	3
<b>3. Results and Analysis</b>	<b>4</b>
3.1 High-Speed Footage Analysis .....	4
3.2 Postimpact Photo Analysis .....	4
3.3 Ceramic Mass Loss Calculation .....	5
<b>4. Conclusions</b>	<b>5</b>
<b>Appendix A. Data Summary</b>	<b>15</b>
<b>Appendix B. Post Impact Photographs: Back Surface</b>	<b>17</b>
<b>Distribution List</b>	<b>19</b>

---

## List of Figures

---

Figure 1. Schematic of the target configurations. ....	6
Figure 2. Schematic of range setup (not to scale). ....	6
Figure 3. Measurement of the total crack length of a 50-mm flat-to-flat hex tile using Image-Pro Plus 6.3. ....	7
Figure 4. Measurement of the area of the remaining ceramic of a 50-mm flat-to-flat hex using Image-Pro Plus 6.3. ....	8
Figure 5. Total crack lengths for each target. ....	9
Figure 6. Remaining ceramic area for each target. ....	10
Figure 7. Average total crack length/remaining ceramic area for each target. ....	11
Figure 8. Average total crack length/original area for each target. ....	12
Figure 9. Average mass loss for each target type. ....	13
Figure B-1. 100-mm flat-to-flat. ....	18
Figure B-2. 75-mm flat-to-flat. ....	18
Figure B-3. 50-mm flat-to-flat. ....	18

---

## List of Tables

---

Table 1. Summary of mass, velocity, and pressure for each shot. ....	13
Table A-1. Summary of data. ....	16

---

## **Acknowledgments**

---

I would like to thank George Washington University and the Science and Engineering Apprenticeship Program for funding this research. I would also like to thank the following people for helping and supporting my project: Shane Bartus, Pat Swoboda, Matthew Burkins, Lynn Maclary, Brian Leavy, Dick Mudd, Jeff Ball, Bob Borys, Colby Adams, Jim Wolbert, Terrance Taylor, Ronald Worthington, Michael Blount, Denver Gallardy, Michael Zellner, Donnie Little, Phil Davis, and Dave Churn.

INTENTIONALLY LEFT BLANK.

---

## 1. Introduction

---

Ceramics are currently being investigated because they have desirable characteristics for armor such as high compressive strength, high hardness and low density.<sup>1</sup> The role of ceramics in armors is to break up, erode, and, in turn, defeat the penetrator.

When a penetrator strikes a ceramic, it tends to deform or mushroom at the point of contact. Sometimes, depending of the penetrator material, it erodes or dwells on the ceramic front surface before penetrating into the tile.<sup>2,3</sup> When the entire penetrator dwells on the ceramic surface without appreciable penetration, the phenomenon is termed interface defeat.<sup>1</sup> The fractured ceramic in contact with the projectile is called the comminuted zone. The ceramic fragments interlock together under the high pressure from the projectile and the comminuted area remains elastic until a critical load is reached. Dwell is when the projectile cannot penetrate the ceramic while the comminuted area is elastic. After the critical load is reached, the load-bearing capacity of the ceramic decreases, and the projectile penetrates the ceramic.

Interface defeat typically occurs at relatively low velocities. As the projectile velocity increases, the dwell time decreases and the projectile begins to penetrate into the ceramic. The velocity where a projectile changes from interface defeat to penetration is called the dwell-penetration transition velocity.<sup>3</sup>

Interface defeat can occur at high velocities if there is a buffer in front of the ceramic or the ceramic is confined and under prestress.<sup>3</sup> Confinement devices are typically made of metal and have an opening to enclose the ceramic. The circumference or perimeter of the ceramic is larger than the opening, and the ceramic must be forced into the confinement or the confinement should be expanded using heat. Confinement and prestress improves ballistic performance because it keeps the ceramic fragments together during impact instead of allowing failed material to move out of the way of the projectile. Prestress may also elevate the pressure required to initiate ceramic failure.

After a projectile strikes the ceramic, a compressive wave from the impact travels through it. The wave reflects off the back plate as a tensile wave because of the difference in impedances of the two materials. The amount of damage increases as the difference between the impedances of the back plate and the ceramic increases. The tensile wave causes damage and the formation of cracks. The cracks create a cone with a base on the back of the tile and a nose where the

---

<sup>1</sup> Hauver, G. E.; Rapacki, E. J., Jr.; Netherwood, P. H.; Benck, R. F. *Interface Defeat of Long-Rod Projectiles by Ceramic Armor*; ARL-TR-3590; U.S. Army Research Laboratory: Aberdeen Proving Ground, MD, September 2005.

<sup>2</sup> Chen, W.; Rajendran, A. M.; Song, B.; Nie, X. Dynamic Fracture of Ceramics in Armor Applications. *J. Am. Ceram. Soc.* **2007**, *90* (4), 1005–1018.

<sup>3</sup> Holmquist, T. J.; Anderson, C. E., Jr.; Behner, T.; Orphal, D. L. Mechanics of Dwell and Post-Dwell Penetration. *Adv. Appl. Ceram.* **2010**, *109* (8), 467–479.

projectile is in contact with the ceramic. The projectile tries to penetrate the ceramic until it loses all of its kinetic energy; if it has enough energy, it will perforate the ceramic. Meanwhile, the back plate and the ceramic begin to bend, which cause more tensile stress and ceramic failure.

Moreover, the ballistic performance of ceramics depends on several factors from the velocity and shape of the projectile to the hardness, density, and shape of the ceramic tile.<sup>4</sup> For example, thicker ceramic tiles tend to not suffer as much damage as thin ceramics. They fail differently from thin ceramics; failed ceramic material flows outward in the opposite direction that the projectile is moving.<sup>2</sup> The flowing ceramic particles erode the penetrator while cracks propagate through the ceramic. After the impact, a tunnel with a diameter slightly larger than the diameter of the projectile is left behind.

Although it is known that thicker ceramics perform better ballistically than thinner ceramics, little is known about how the size (area) of the ceramic tiles affects ballistic performance. Also, additional data need to be collected to more accurately model the ballistic response of ceramics. Because of the stochastic nature of brittle ceramic materials, material model development is difficult.

The purpose of this study was to investigate whether the size of the ceramic tile affects how much damage it suffers. The data from this study can give more insight on the ballistic performance of ceramics, armor design, and could be used for modeling.

---

## 2. Materials and Methods

---

For this study, targets were created using different sized ceramic tiles. The targets were shot with a gas gun while a high-speed camera captured the crack growth. The high-speed camera footage, postimpact pictures, and the remaining mass of the target were used to analyze and assess which size ceramic tile had the most damage.

### 2.1 Target Setup

Three different sizes of 19-mm-thick hexagonal tiles of SiC-X1 (Coors-Vista Advanced Ceramics) were used for the targets. The sizes were 50-, 75-, and 100-mm flat-to flat, as shown in figure 1. The ceramic tiles were adhered to 152.4 × 152.4 mm × nominally 12.7-mm-thick polycarbonate backing plates using 0.635-mm-thick Deerfield Thermoplastic Polyurethane (TPU) as shown in figure 1.

The ceramic was adhered to the polycarbonate backing plate by 0.635-mm-thick TPU pieces with the same dimensions as the ceramic tile. Next, the target assembly was put under a vacuum bag and placed under a vacuum. Finally, the vacuum-bagged target was put into an oven that was

---

<sup>4</sup> Sherman, D. Impact Failure Mechanisms in Alumina Tiles on Finite Thickness Support and the Effect of Confinement. *International Journal of Impact Engineering* **2000**, *24*, 313–328.

heated to 104.4 °C for 8.5 h. The oven melted the TPU that joined the ceramic to the polycarbonate backing plate while remaining transparent. An unobstructed view of the distal ceramic face was needed for data collection. Nine targets were constructed, three targets for each ceramic geometry.

## **2.2 Light Gas Gun Setup**

A 27.7-mm bore light gas gun was used to launch 12.7-mm diameter spheres at the targets. Each sphere was composed of tungsten carbide (WC) with a 6% cobalt binder and weighed 16 g. The projectiles' velocity was  $440 \pm 5.6$  m/s. Two flash x-rays were set up above the shot line in front of the light gas gun to measure the velocity of the projectile prior to impact.

The targets were clamped to a metal stand and aligned with a laser to the gun's shot line. The light gas gun used compressed helium to propel the launch package which consisted of a WC sphere that was embedded in a hole with a depth equal to the projectile radius in a 2.41 cm long, high-density polyurethane foam sabot. A sabot stripper on the muzzle of the gun disengaged the sabot from the sphere prior to velocity measurement and interaction with the target (figure 2). Prior to the shots, the mass of the launch package was measured (see table 1). It was important that the masses were consistent to achieve a constant velocity. The projectile traveled from the gun, through a break screen which triggered two flash x-rays, and through a second break screen on the front of the target before hitting the ceramic. The second break screen triggered the high-speed camera, which was set up behind the target and protected by a piece of polycarbonate. The high-speed camera footage was analyzed using Phantom Camera Software and Image-Pro Plus 6.3 to quantify and qualify the ceramic damage as a function of time after impact. Also, postimpact photographs of the front and back of the target were taken.

## **2.3 Data Analysis**

The high-speed footage was analyzed frame by frame with Phantom software to qualify the damage. The propagation of radial cracks and the formation of peripheral fragments were observed.

The postimpact pictures were analyzed with Image-Pro Plus 6.3 to quantify the distal ceramic damage by measuring the total crack length as shown in figure 3. The length of all the cracks were measured and added together and are listed in appendix A. The area of the remaining ceramic on the back plate was also measured, figure 4. The crack density, which is equal to the total crack length divided by the area of the ceramic, was calculated to quantify the damage on the ceramic. Higher crack densities are indicative of more damage than smaller crack densities. This methodology only captures the distal surface damage of the ceramic.

Next, the mass loss of the ceramic was calculated by subtracting the remaining mass from the original mass of the targets. The components of each type of target were weighed and the masses were added together to find the original mass of the targets. After the targets were shot, they were weighed and it was assumed that the mass loss from the polycarbonate and TPU was negligible.

---

### 3. Results and Analysis

---

#### 3.1 High-Speed Footage Analysis

The high-speed camera footage, taken at 32  $\mu\text{s}$ /frame, showed that radial cracks within the ceramic started to propagate through the ceramic thickness in all the targets after projectile touchdown on the ceramic surface (within the camera framing rate). For the 100-mm flat-to-flat, the radial cracks were completely done propagating for all the targets within 64–97  $\mu\text{s}$  (2–3 frames) after touchdown.

There was more variability for the time it took for the radial cracks to finish propagating in the 75-mm flat-to-flat. For two out of the three 75-mm flat-to-flat ceramics, the radial cracks stopped growing after 32–33  $\mu\text{s}$  (one frame). The cracks in the third 75-mm flat-to-flat ceramic took 97  $\mu\text{s}$  to finish propagating.

The radial crack propagation for the 50-mm flat-to-flat took 32–64  $\mu\text{s}$  (1–2 frames) to finish growing. The 50-mm flat-to-flat ceramics had more radial cracks than the 100-mm flat-to-flat and 75-mm flat-to-flat ceramics.

All the targets had large peripheral fragments. In the 100-mm flat-to-flat ceramics, the peripheral fragments started to form after the radial cracks stopped growing, whereas peripheral cracks started to form while the radial cracks grew in both the 50- and 75-mm flat-to-flat tiles. The fragments in the 75- and 100-mm flat-to-flat ceramics, for the most part, stayed attached to the polycarbonate back plate. However, for the 50-mm flat-to-flat ceramics, the fragments came off the polycarbonate, reducing the amount of remaining ceramic. These fragments are probably the result of the compression wave reflecting off the edge of the ceramic, which is a free surface.

#### 3.2 Postimpact Photo Analysis

The postimpact photo analysis supports what was seen with the high-speed imagery and still images are included in appendix B. The crack measurements showed that the 100-mm flat-to-flat ceramic had the longest total crack length, and the 50-mm flat-to-flat ceramic had the shortest total crack length. Similarly, the 100-mm flat-to-flat had the largest remaining ceramic area, and the 50-mm flat-to-flat had the least remaining ceramic area (see figures 5 and 6). Figure 7 shows the average crack length/remaining ceramic area for each size ceramic tile, while figure 8 shows the average crack length/original ceramic area. Both of the figures show that the 50-mm flat-to-flat had the largest total crack density, while the 100-mm flat-to-flat had the lowest crack density.

### **3.3 Ceramic Mass Loss Calculation**

The amount of ceramic loss is shown in figure 9. The average ceramic mass loss for 50-mm flat-to-flat tiles was 94.0%, while the average ceramic loss for the 75-mm flat-to-flat and the 100-mm flat-to-flat were 73.4% and 62.6%, respectively. This indicates, again, that the 50-mm flat-to-flat ceramic suffered the most damage.

---

## **4. Conclusions**

---

Three different dimensioned 19-mm-thick SiC-X1 ceramic targets (50-, 75-, and 100-mm flat-to-flat) were impacted with a 12.7-mm-diameter tungsten carbide spheres to study whether the size of a ceramic affects the damage that occurs during a ballistic impact. It was concluded that the 50-mm flat-to-flat had the highest damage density. However, the difference in crack density was less pronounced when comparing the 75- and 100-mm flat-to-flat ceramics. A ceramic's size appears to affect the amount of damage that occurs. Smaller ceramic tiles appear to suffer more damage than larger ceramic tiles when both are struck by a projectile traveling at the same velocity, but more testing needs to be done to confirm this trend. If this trend does prove to be true, then it can be used to improve future computer models for ballistic impacts into ceramic and aid armor designers in improving single and multiple impact armor design.

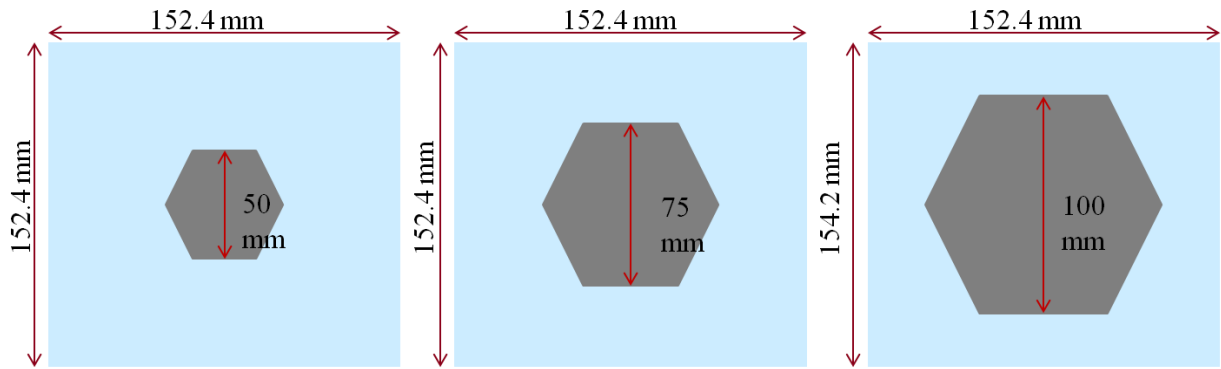


Figure 1. Schematic of the target configurations.

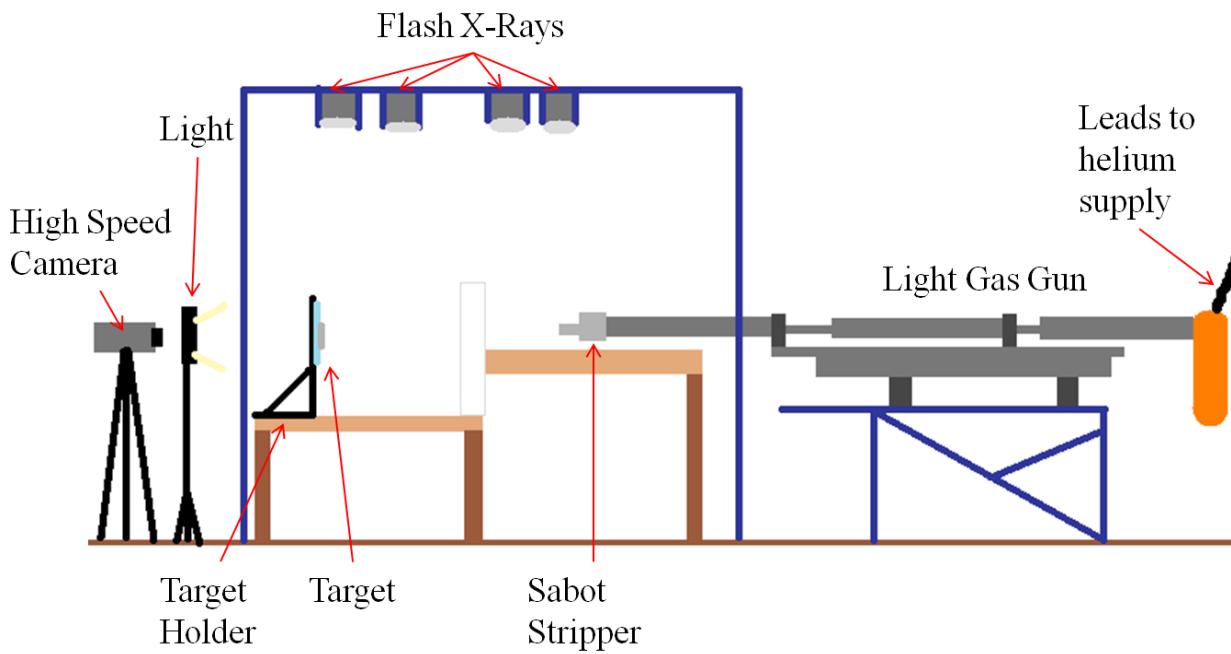


Figure 2. Schematic of range setup (not to scale).

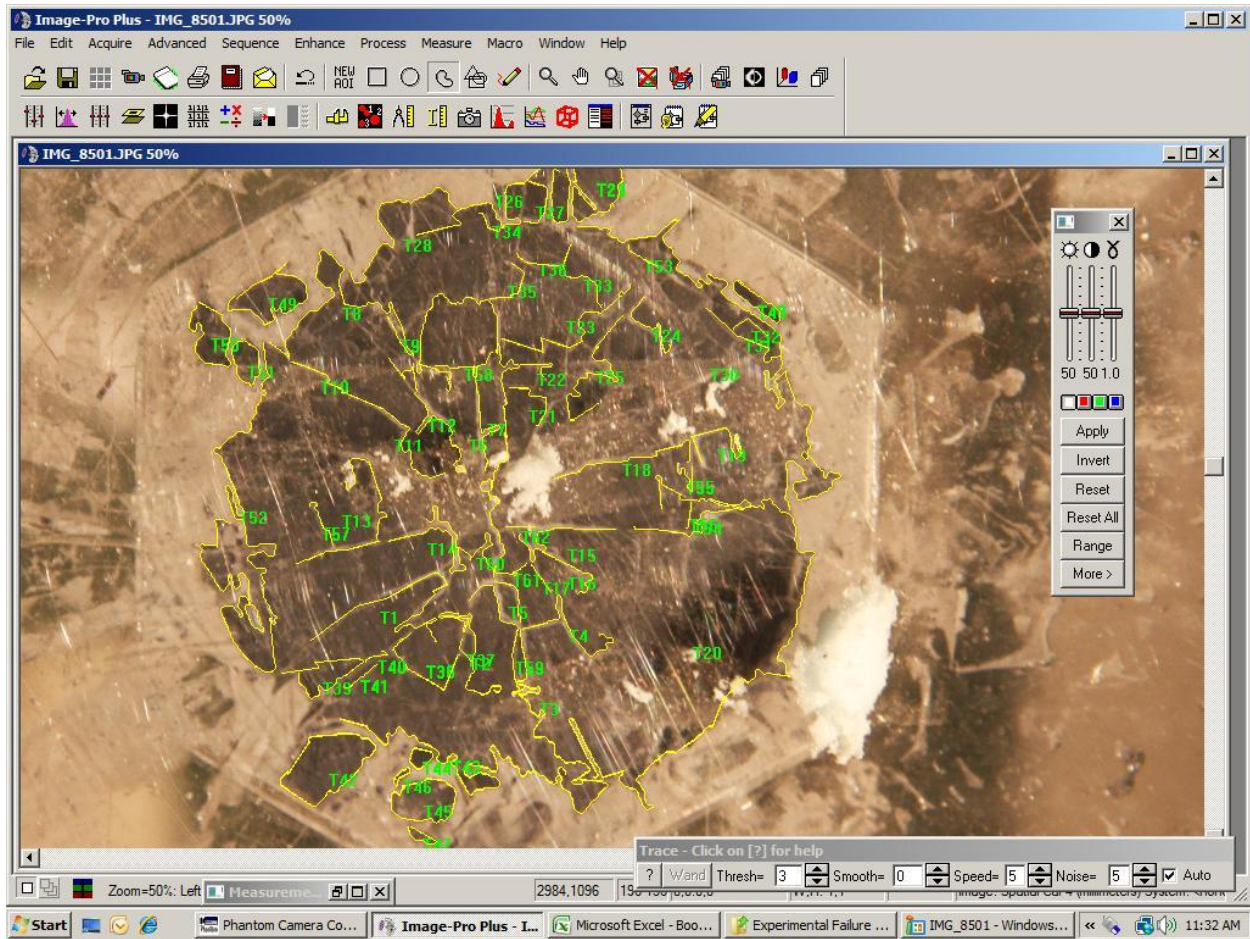


Figure 3. Measurement of the total crack length of a 50-mm flat-to-flat hex tile using Image-Pro Plus 6.3.

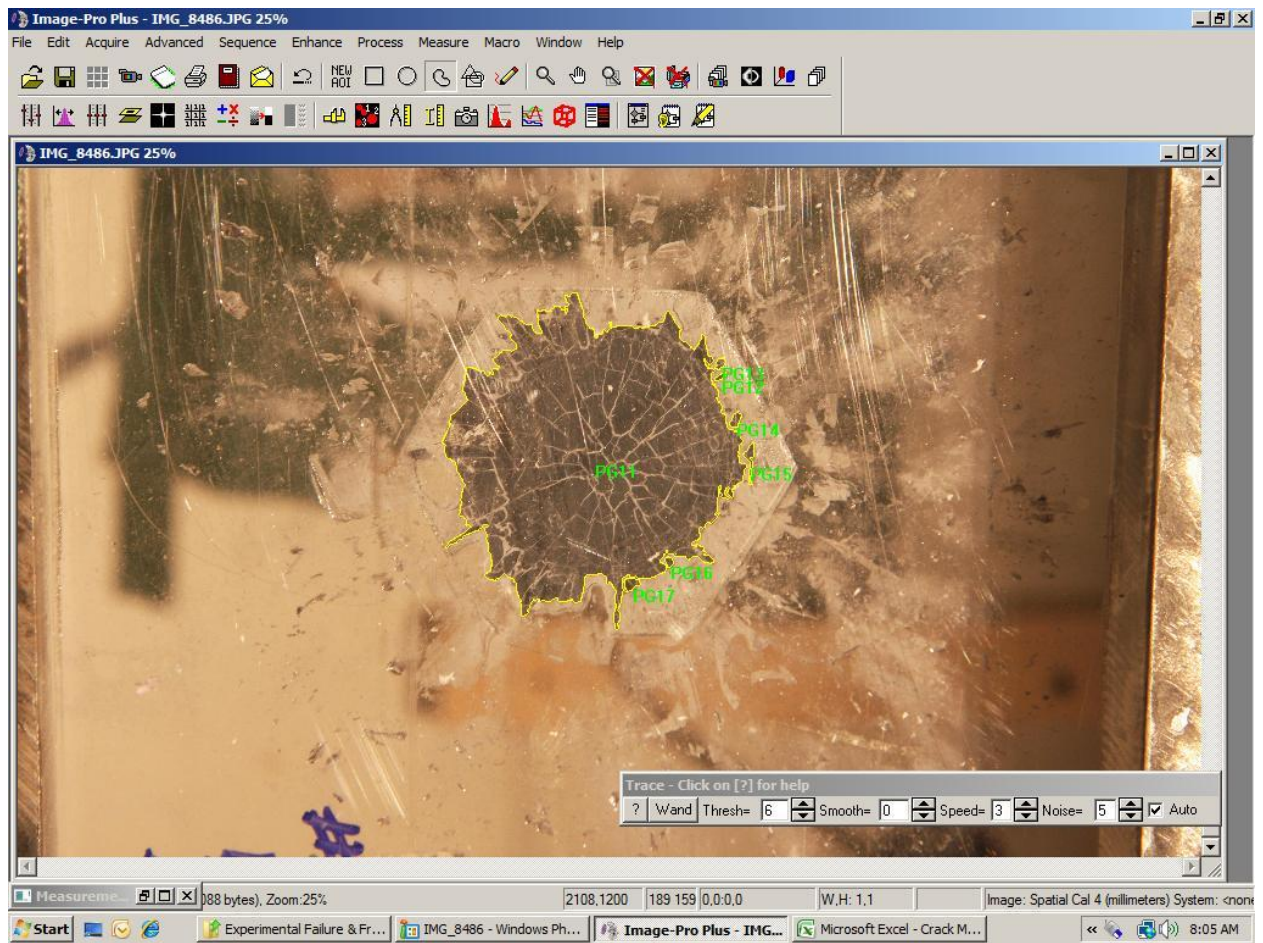


Figure 4. Measurement of the area of the remaining ceramic of a 50-mm flat-to-flat hex using Image-Pro Plus 6.3.

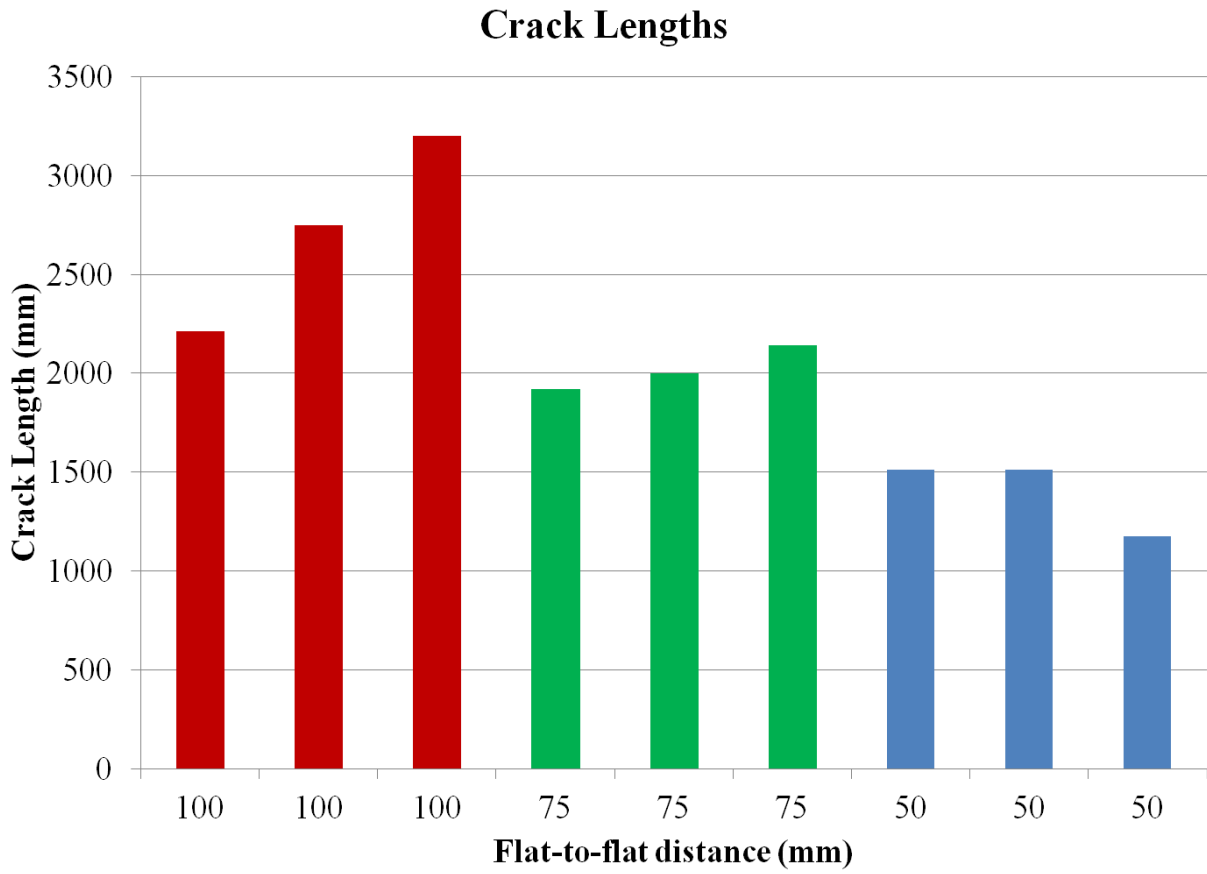


Figure 5. Total crack lengths for each target.

## Remaining Ceramic Area

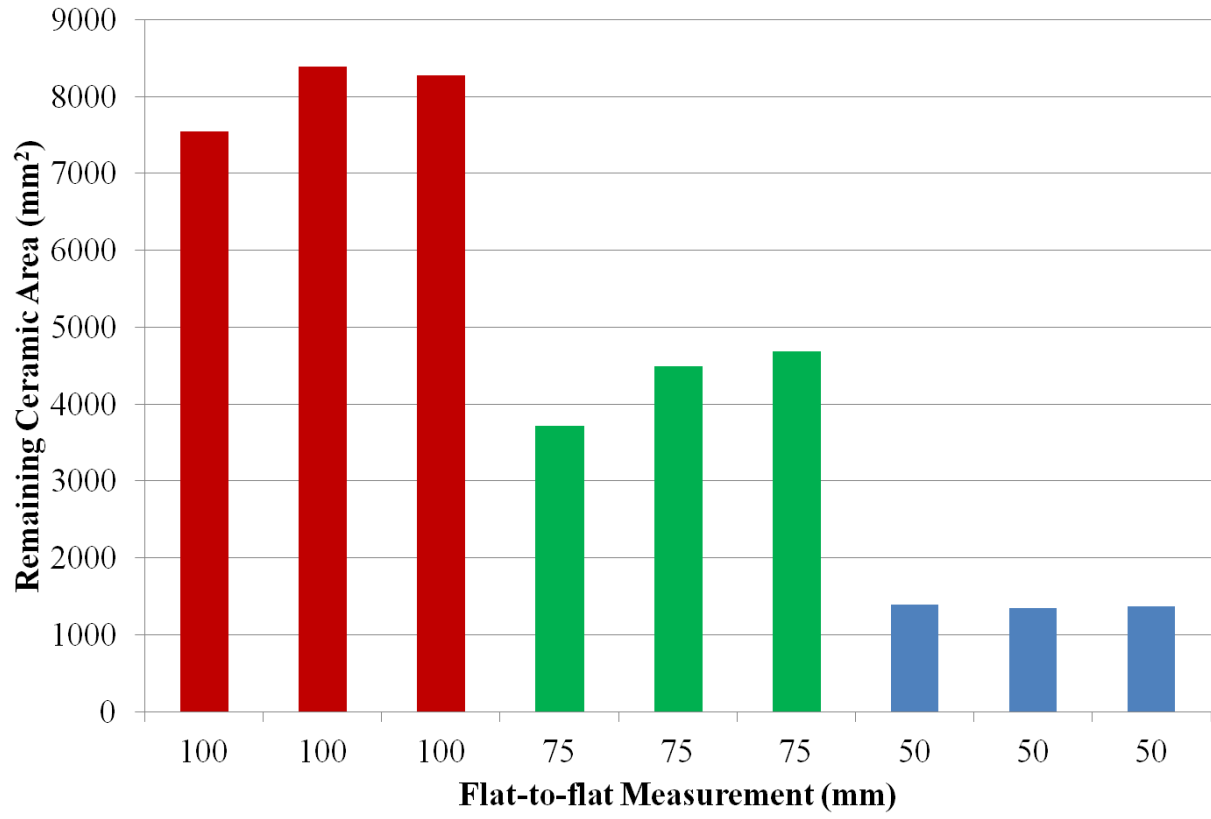
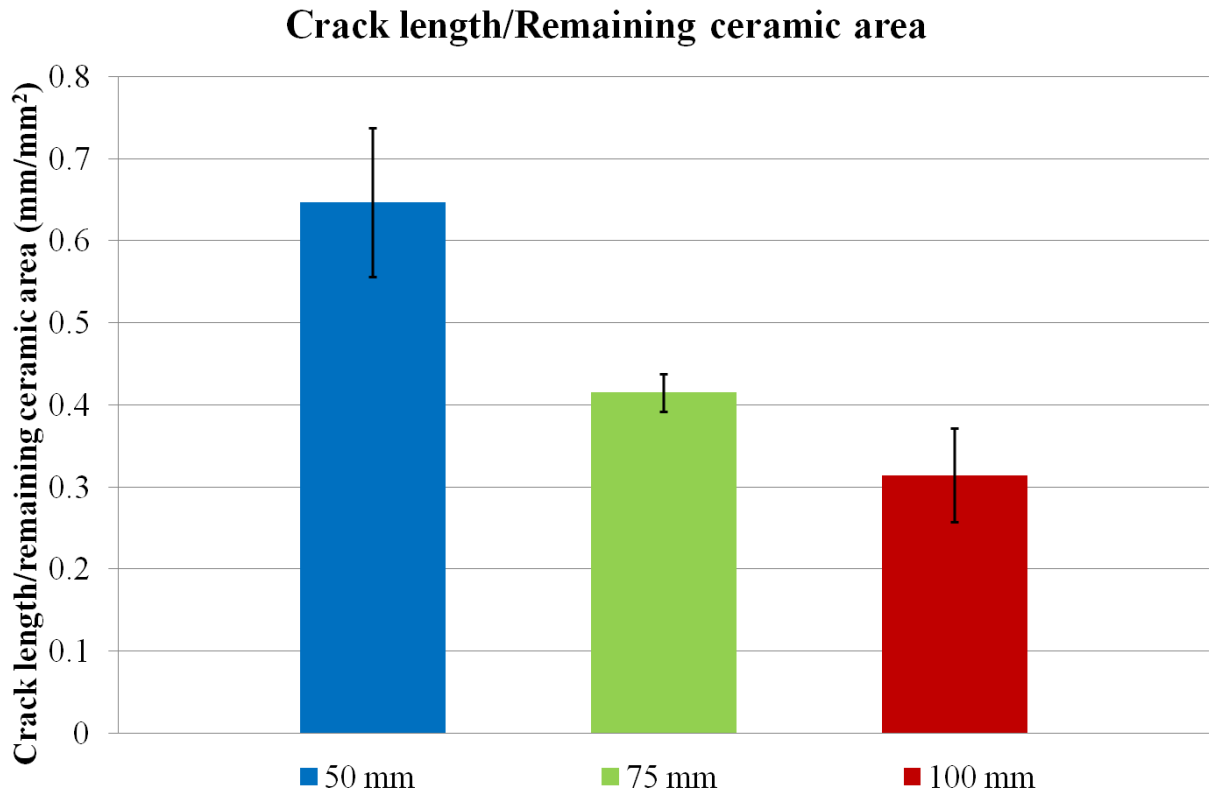
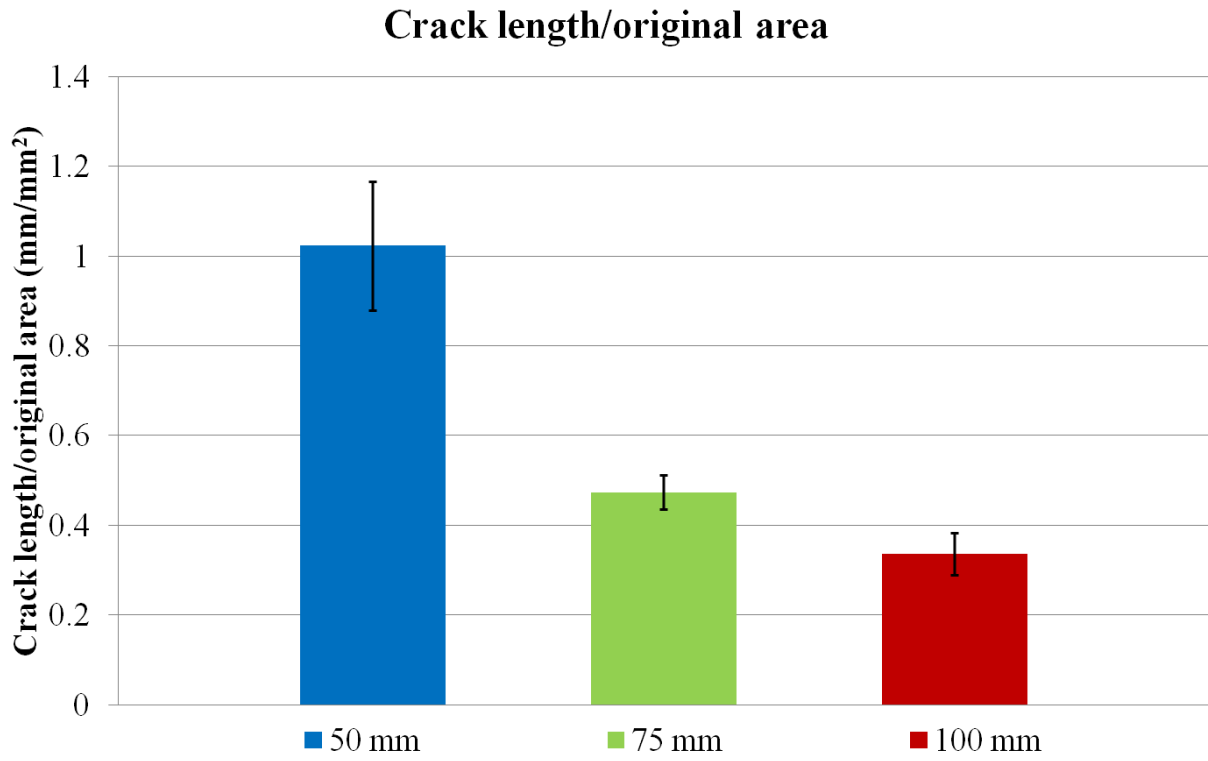


Figure 6. Remaining ceramic area for each target.



**Flat-to-flat measurement**  
Figure 7. Average total crack length/remaining ceramic area for each target.



#### Flat-to-flat measurement

Figure 8. Average total crack length/original area for each target.

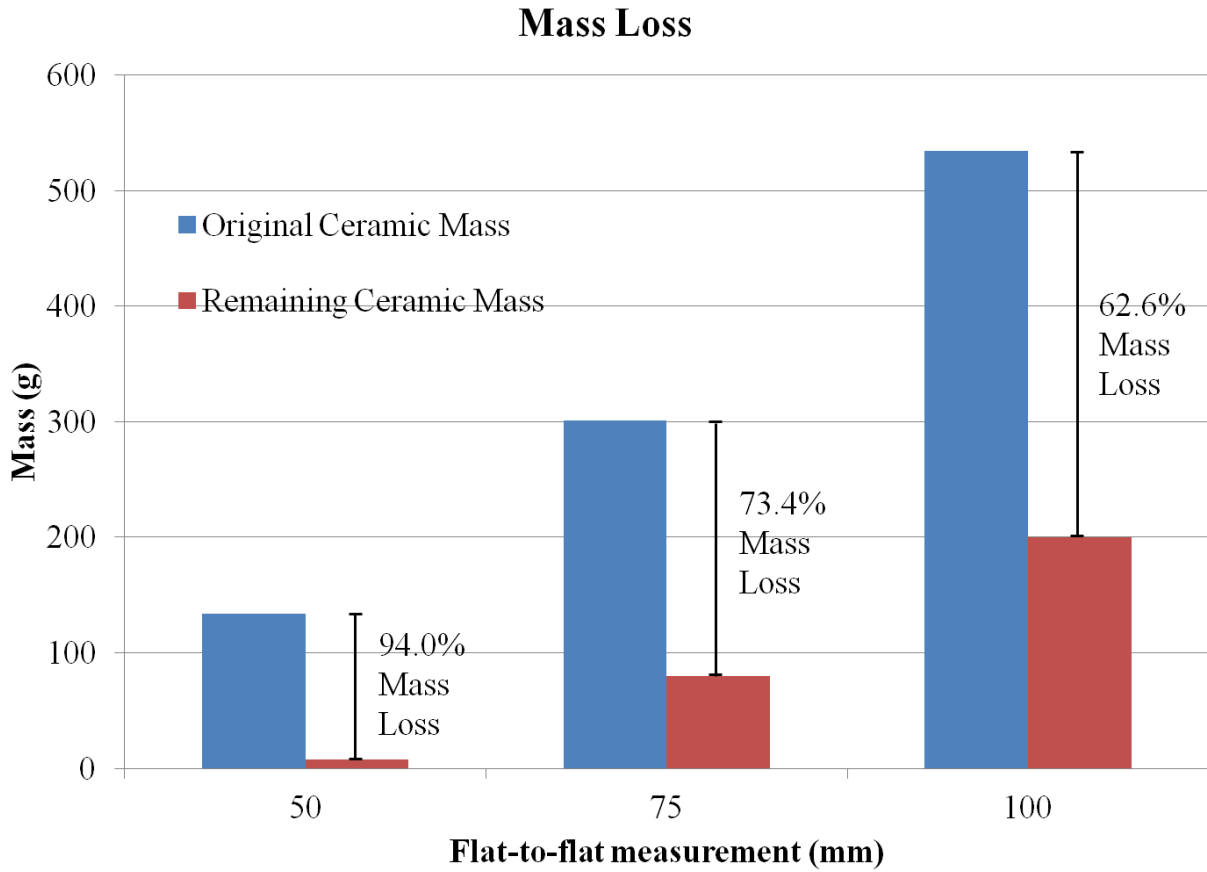


Figure 9. Average mass loss for each target type.

Table 1. Summary of mass, velocity, and pressure for each shot.

Shot No.	Ceramic Flat-to-Flat Distance (mm)	Launch Package Mass (g)	Actual Velocity (m/s)	Actual Pressure (kpa)
28	100	22.2	438	5033.2
29	100	22.1	439	5033.2
30	100	22.1	No velocity measurement; x-ray pre-triggered	5033.9
31	75	22.1	429	5034.6
32	75	22.1	437	5044.2
33	75	22.1	428	5037.3
34	50	22.1	436	5074.5
35	50	22.1	446	5041.5
36	50	22.1	441	5041.5

INTENTIONALLY LEFT BLANK.

---

## **Appendix A. Data Summary**

---

Table A-1. Summary of data.

<b>Flat-to-Flat (mm)</b>	<b>Crack Length (mm)</b>	<b>Area (mm<sup>2</sup>)</b>	<b>Original Area (mm<sup>2</sup>)</b>	<b>Crack Length/Original Area (mm/mm<sup>2</sup>)</b>	<b>Standard Deviations</b>	<b>Crack Length/Area (mm/mm<sup>2</sup>)</b>	<b>Standard Deviations</b>
100	2212	7549	8660	0.255	—	0.293	—
100	2747	8383	8660	0.317	—	0.327	—
100	3199	8271	8660	0.369	0.057	0.386	0.047
75	1920	3718	4871	0.394	—	0.516	—
75	2001	4487	4871	0.410	—	0.446	—
75	2143	4687	4871	0.440	0.023	0.457	0.037
50	1513	1388	2165	0.699	—	1.090	—
50	1513	1351	2165	0.699	—	1.119	—
50	1173	1366	2165	0.542	0.090	0.858	0.142

---

**Appendix B. Post Impact Photographs: Back Surface**

---



Figure B-1. 100-mm flat-to-flat.



Figure B-2. 75-mm flat-to-flat.



Figure B-3. 50-mm flat-to-flat.

NO. OF  
COPIES ORGANIZATION

1 DEFENSE TECHNICAL  
(PDF) INFORMATION CTR  
DTIC OCA

2 DIRECTOR  
(PDF) US ARMY RESEARCH LAB  
RDRL CIO LL  
IMAL HRA MAIL & RECORDS MGMT

1 GOVT PRINTG OFC  
(PDF) A MALHOTRA

1 COORSTK VISTA  
(PDF) R PALICKA

2 SANDIA NATL LABS  
(PDF) O ESTRAC  
J NIEDE

2 SOUTHWEST RSRCH INST  
(PDF) J WALKER  
C ANDERSON

1 3M  
(PDF) M NORMANDIA

33 DIR USARL  
(PDF) RDRL LOA  
S YOUNG  
RDRL WML H  
T EHLERS  
L MAGNESS  
RDRL WMM A  
J WOLBERT  
RDRL WMM B  
R CARTER  
B LOVE  
RDRL WMM D  
L VARGAS  
S WALSH  
RDRL WMM E  
J CAMPBELL  
J LASALVIA  
J SWAB  
RDRL WMP A  
J BALL  
R MUDD

NO. OF  
COPIES ORGANIZATION

RDRL WMP B  
C HOPPEL  
S SATAPATHY  
T WEERASOORIYA

RDRL WMP C  
T BJERKE  
R LEAVY  
C WILLIAMS  
R WORTHINGTON

RDRL WMP E  
M BURKINS  
B CHAMISH  
D GALLARDY  
D HACKBARTH  
D HORNBAKER  
E HORWATH  
J HOUSKAMP  
T JONES  
M KORNECKI  
C KRAUTHAUSER  
D LITTLE  
K MCNAB  
P SWOBODA

1 DSTL  
(PDF) A COOK

INTENTIONALLY LEFT BLANK.